Introduction

This article reports on the extension of the existing PHOENICS VOF (volume of fluid) option to simulate three phase flows, such as those encountered in applications involving three different immiscible fluids. Examples include systems involving combinations of liquids and gases with differing densities, like those found in the water/oil/air interfaces of an oilfield separator and the liquid-steel/liquid-slag/gas interfaces of a gas-stirred metallurgical ladle. The extension to three fluids involves the solution of a conservation for an additional colour (or indicator) function, C_3, to represent the third phase; and a modification of the surface-tension force in the mixture momentum equation to handle the three distinct fluids.

The PHOENICS 3-phase VOF implementation is tested by its application to two rising bubble cases, one for a bubble rising in a liquid column, and the other for a bubble rising in a column with two stratified liquids. The first case is important for verifying that the VOF extension produces results that are in agreement with published numerical results for the simpler two-phase system. The second test case is qualitative in the sense that it simulates a full three-phase system to investigate the bubble rise in response to changes in the physical properties of each phase.

Theoretical Considerations

The transport equation for C_3 has the same form as the existing colour function C_1 used in two-phase VOF simulations, i.e.:

$$\frac{\partial C_3}{\partial t} + \nabla \cdot V C_3 = 0 \qquad\qquad (1)$$

The option exists in PHOENICS to solve this equation in conservative or in non-conservative form, depending on the physical problem. The following algebraic equation enforces volume continuity and links the two colour functions: $\sum_{n=1}^{3} C_n = 1$, where C_n is the colour function of phase n.

The **physical properties** of the resulting mixture are computed under the above constraint by using equations of the form: $\phi = \sum_{n=1}^{3} C_n \phi_n$, where ϕ denotes the density, kinematic viscosity, specific heat capacity, thermal conductivity and volumetric expansion coefficient

The PHOENICS two-phase VOF method uses the standard continuous surface force (CSF) approach of Brackbill et al (1992) to introduce **surface-tension forces** into the momentum equations in form of an equivalent body force, which in case of a two-phase system, takes the following form: $\mathbf{f}_{cap} = \sigma \kappa_i \delta \mathbf{n}_i$, where σ is interfacial tension, $\mathbf{n}_i = -\nabla C_i / |\nabla C_i|$ is unit normal vector at the interface pointing out of the i-phase, with C_i the colour function of the i-phase, $\delta = |\nabla C_i|$ is the Dirac delta function centred at the interface and $\kappa_i = -(\nabla \cdot \mathbf{n}_i)$ is the interface curvature.

The drawback of the CSF approach is that for different densities of adjacent phases, the capillary force introduced into the momentum equations produces an unsymmetrical distribution of the acceleration field relative to the interface location. For example, the acceleration $\mathbf{f}_{cap}/\rho$, where ρ is the local VOF phase density, is much higher in a less dense phase and vice versa. The CSF approach will lead to a thinning or thickening of the smooth transitional region between phases, depending on the direction of the vector $\mathbf{f}_{cap}$. If $\mathbf{f}_{cap}$ is pointing into a less dense phase, then the interface tends to thicken with time, whereas if it is pointing into a denser phase, the interface will become thinner with time. This problem has been resolved by Brackbill et al (1992) for two-phase systems by using density scaling of the CSF (DS-CSF), as follows:

$$f_{cap} = -\sigma \kappa_i \nabla C_i \frac{\rho}{\langle \rho \rangle} \tag{2}$$

where $\langle \rho \rangle = (\rho_1 + \rho_2)/2$ is the average density between adjacent phases 1 and 2. This practice results in a symmetric distribution of the acceleration with respect to the interface.

In this work, by following Tofighi and Yildiz (2013), the DS-CSF has been extended to three phases by splitting the resulting capillary force into three constituents, one per phase. Each of these phase-specific forces is given zby equation (2) above, but instead of using interfacial surface tensions, three phase-specific surface tensions σ_n (where n = 1,2, 3) are used in these forces. This approach is valid only for three-phase systems, as will be discussed later. When focusing on a given phase n, the idea of density scaling is to treat the two others as a single n-adjacent phase with spatially varying density.

By analogy with a two-phase system, but using now the density of the n-adjacent phase for the DS-CSF, the capillary force for a three-phase system can be computed as:

$$f_{cap} = \sum_{n=1}^{3} f_{ncap} = -\sum_{n=1}^{3} \sigma_n \kappa_n \nabla C_n \frac{\rho}{\langle \rho \rangle_\alpha} \tag{3}$$

where $\mathbf{f}_{n,cap}$ is the equivalent of $\mathbf{f}_{cap}$ for phase n with $\langle \rho \rangle_n = (\rho_n + \rho_{n\text{-adjacent}})/2$. This formulation redistributes the surface forces across interfaces in such a way as to produce a symmetric acceleration. It remains to define the values of phase-specific surface tensions. The idea is based on the decomposition of the resulting force vector into three constituent phase-specific forces (see Tofighi and Yildiz (2013)). These phase-specific forces are then treated individually in the same manner as surface forces in two-phase systems, where only one type of interface is possible. For this purpose, the interfacial tension between phases n and β is expressed through artificially introduced phase-specific surface tensions, so that $\sigma_{n\beta} = \sigma_n + \sigma_\beta$ where:

$$\begin{cases} \sigma_1 = 0.5(\sigma_{12} + \sigma_{13} - \sigma_{23}) \\ \sigma_2 = 0.5(\sigma_{12} + \sigma_{23} - \sigma_{13}) \\ \sigma_3 = 0.5(\sigma_{13} + \sigma_{23} - \sigma_{12}) \end{cases} \tag{4}$$

One difficulty in three phase systems is the possibility of direct contact between all phases. However, these situations are accounted for automatically by the foregoing capillary-force decomposition into the sum of phase-specific capillary forces.

Application to the 2-phase system of a bubble rising in liquid

The flow considered is a two-dimensional bubble rising in a column of liquid, as defined by Hysing et al. (2009) as test case 2. This case is representative of industrial applications because it concerns a bubble with a density much lower than that of the surrounding fluid. The solution domain is illustrated in Figure 1; and the liquid (phase 1) properties are taken as ρ_1=1000 kg/m^3 and μ_1=10 Ns/m^2. The gas (phase 2) properties are set to ρ_2=1 kg/m^3 and μ_2=0.1 Ns/m^2. The surface tension and gravitational acceleration are set to σ=1.96 N/m and g=0.98 m/s^2, respectively.
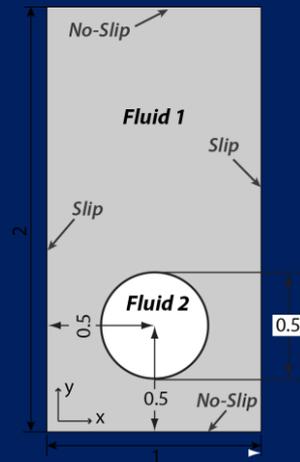
Figure 1. Configuration and boundary conditions for 2d bubble benchmark

The task is to predict the vertical position of the following parameters: the bubble centroid, the bubble rise velocity, the bubble circularity/sphericity, the bubble area and the surface perimeter. The PHOENICS predictions of these parameters are then compared with the numerical results of other workers. The circularity is the inverse ratio of the bubble surface perimeter P_b to the perimeter of the area-equivalent circle in two dimensions P_a. It takes the value of unity at the beginning of the computation and decreases as the bubble deforms.

PHOENICS VOF simulations were performed to cover a time duration 3 seconds using a uniform mesh size h in each coordinate direction, as defined by h =1/40,1/80,1/160 and 320. For comparison, simulations were made using the CICSAM and THINC interface-resolution schemes for discretization of the nonlinear convective term in the transport equation for the colour function.

The results are presented in Figures 2 to 5. Firstly, Figures 2a and 2b show snapshots of the time evolution of the bubble at grid resolution 320. Figure 3 shows the bubble shape obtained with PHOENICS for a grid resolution 320 at time t = 3s, together with numerical results obtained by Gamet et al (2018) using Interfoam and InterIsoFoam. Figure 4 compares the results obtained for PHOENICS VOF-CICSAM with those obtained using PHOENICS VOF-THINC. This figure shows the centre of mass, the rise velocity and the circularity at grid resolutions of 40, 80, 160 and 320. Figure 5 shows results for PHOENICS VOF-CICSAM compared with results obtained with PHOENICS VOF-THINC for the centre of mass, rise velocity and circularity at resolution 320.
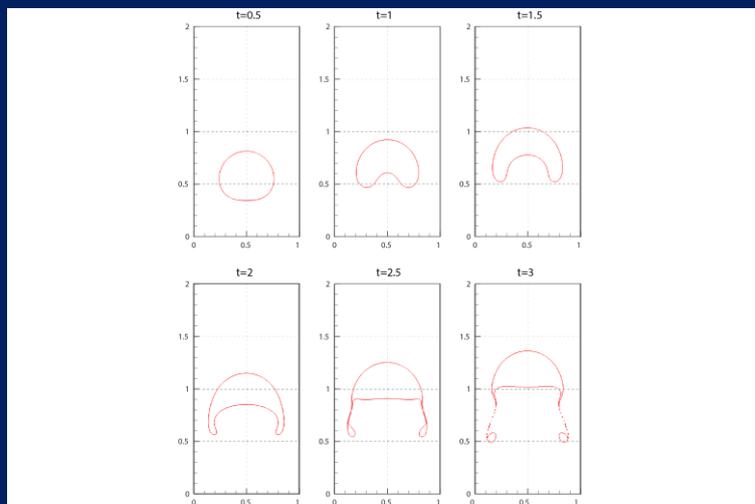

Figure 2a. PHOENICS VOF-THINC: Time evolution of the bubble shape at grid resolution 160×320 (lines contours).
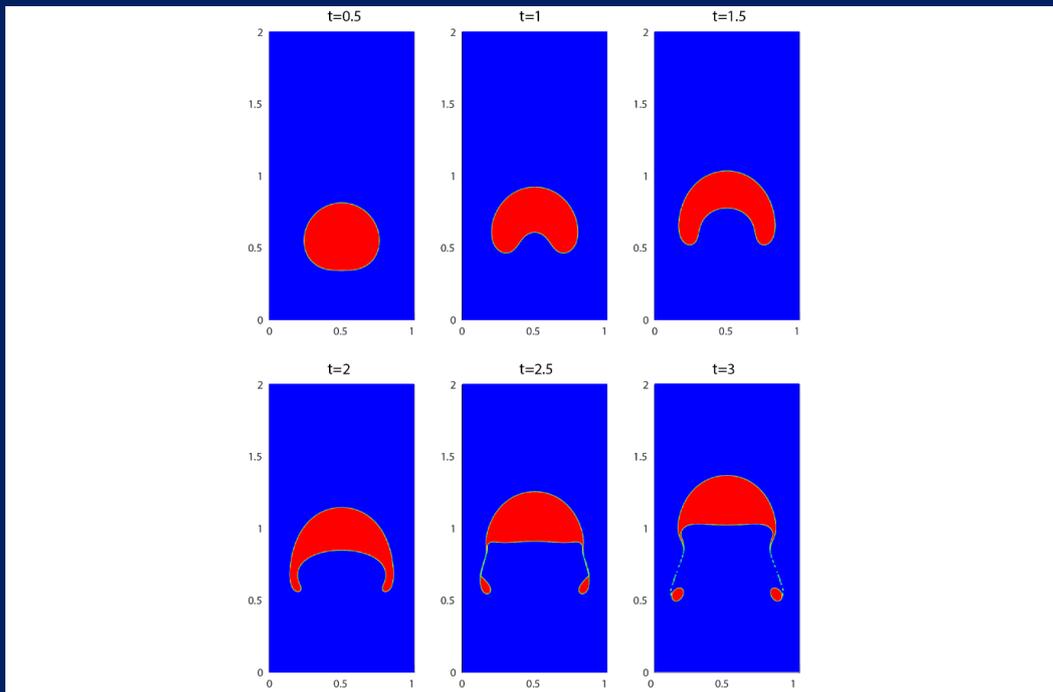
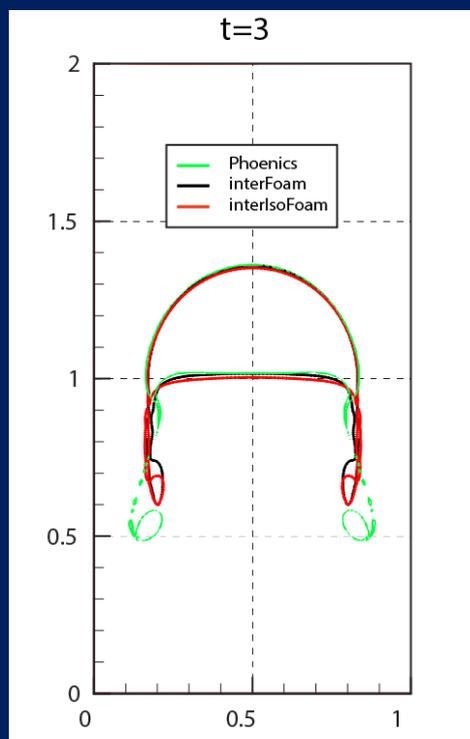**Figure 2b. PHOENICS VOF-THINC: Time evolution of bubble shapes at grid resolution 160×320 (filled colours contours).**

Figure 3. Comparison of bubble shapes at final time t = 3 s for PHOENICS (1/h=320), InterFoam (1/h=160) and InterIsoFoam (1/h=160).
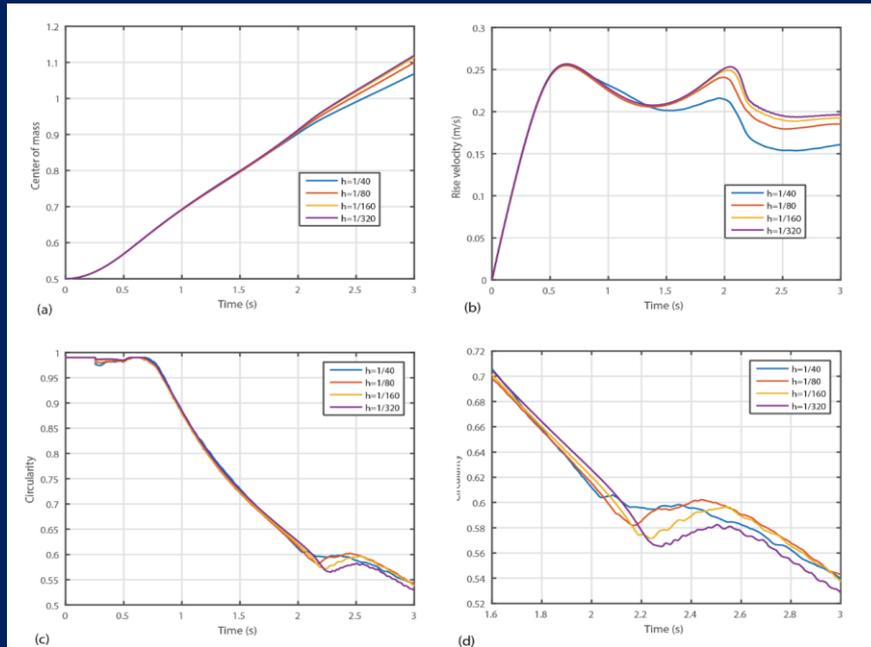
Figure 4. PHOENICS VOF-CICSAM: Time evolution of the centre of mass (a), rise velocity (b), circularity (c) and close-up of the circularity (d) at different grid resolutions.
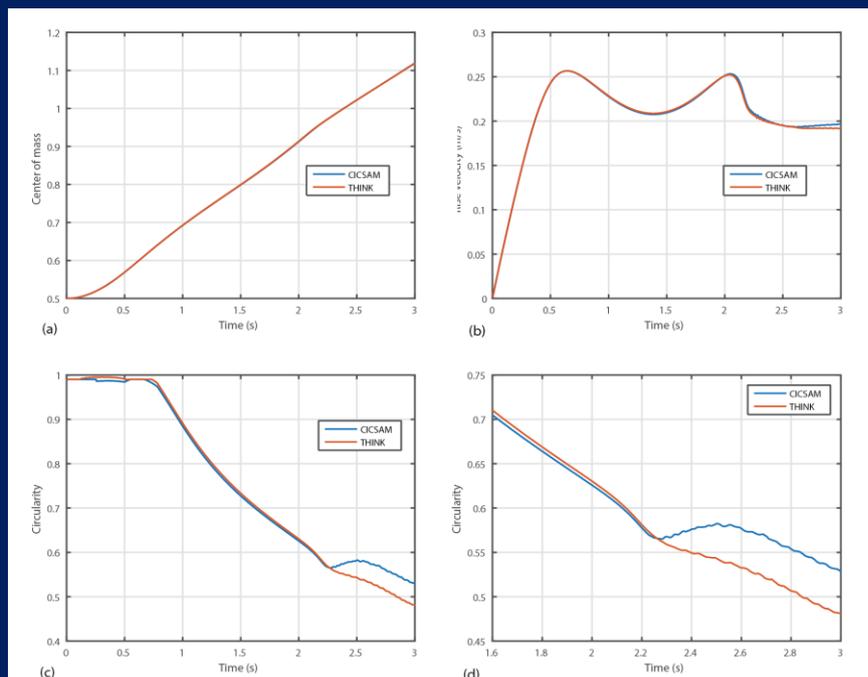

Figure 5. Time evolution of centre of mass (a), rise velocity (b), circularity (c) and close-up of the circularity (d) for PHOENICS VOF-CICSAM (blue) and VOF-THINC (red) at resolution grid 320.

The comparisons reveal the good behaviour of PHOENICS, whether using the CICSAM or THINC VOF method. Moreover, the results compare well with other published results. A thorough study can still be done to investigate the effect of varying several parameters in the PHOENICS VOF method, such as the smoothing level, Dirac function cutoff, number of sweeps, etc.

Application to the 3-phase system of a bubble rising through 2 stratified liquids

In this section, we consider a bubble rising due to buoyancy through two stratified liquids of differing density. The surface tension, viscosity, and gravity are taken into consideration. The computational domain takes a square shape Ω = [0.0, 1.0] × [0.0, 1.0], and at time zero, the bubble (phase 1) has an elliptic shape defined by $\left((x - 0.5)/a\right)^2 + \left((y - 0.325)/b\right)^2 = 1$, with major and minor axes a=0.15 and b=0.075, respectively. Phases 2 and 3 are located above and below the horizontal line y = 0.5 with densities of 1000 and 1500 kg/m^3, respectively.

Gravity acts along the negative vertical direction with magnitude of 9.8 m/s^2. Computations are performed on a 200 × 200 cell grid using three different sets of physical properties, as indicated in Table 1.

Χασε #	Δενσιτψ (κγ/ μ^3)	Δψναμιχ ςισχοσιτιεσ (Πα.σ) (μ_1,μ_2,μ_3)	Συρφαχε τενσιον (N/μ) ($\sigma_{12},\sigma_{13},\sigma_{23}$)
1	(1,1000,1500)	(0.0,1.0,2.0)	(0.5,0.5,1.0)
2	(1,1000,1500)	(0.0,10.0,20.0)	(0.5,0.5,1.0)
3	(1,1000,1500)	(0.0,1.0,2.0)	(50.0,50.0,100.0)

Table 1: Case numbers and physical parameters

The numerical results at four different times (t = 0.02, 0.12, 0.28, 0.5 s) are presented in Figure 6. The bubble rises due to buoyancy, and it can be seen that its shape tends to break up as it moves upwards. This is because the surface force isn't large enough to maintain the circular shape. The effects of viscosity attenuate the rising velocity of the bubble, as well as its shape.
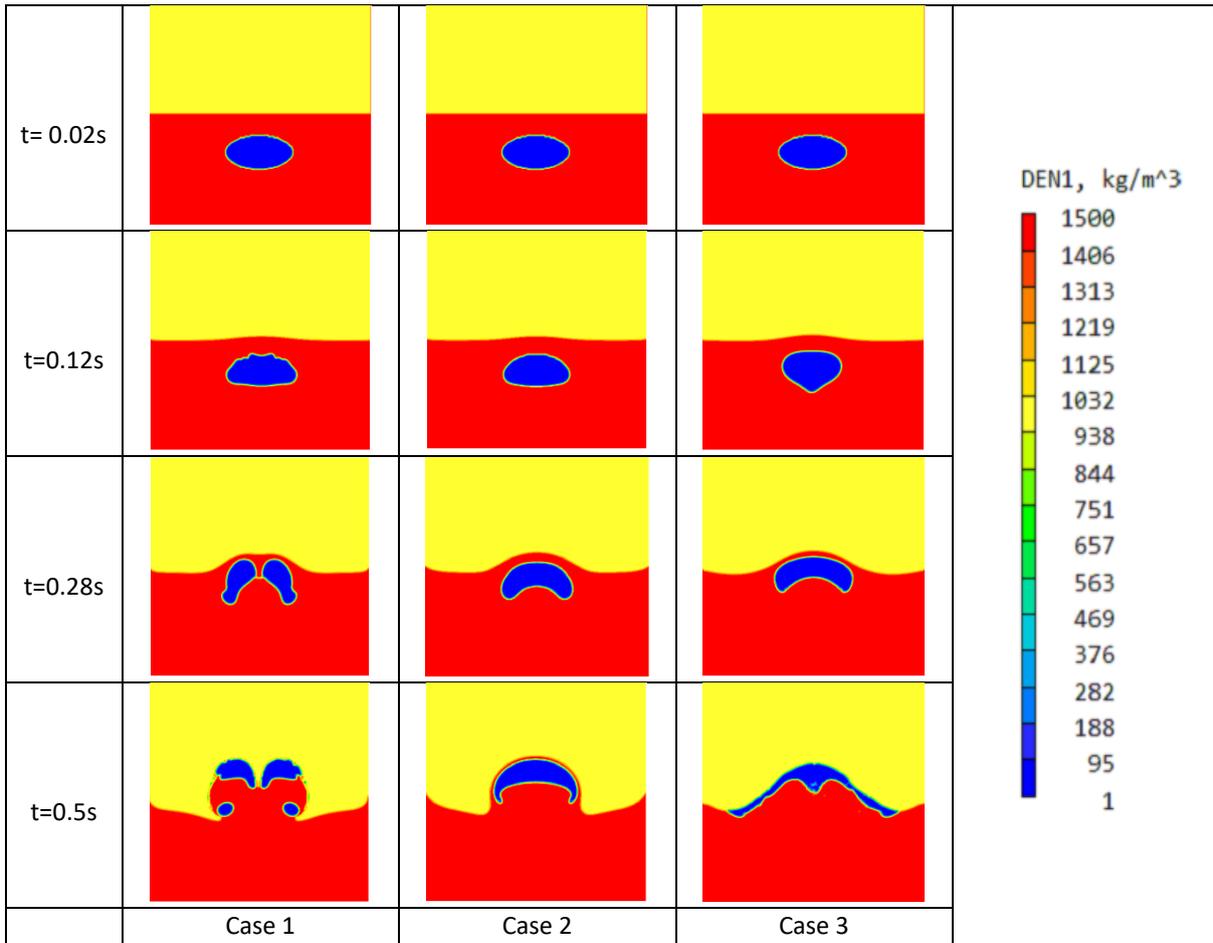
Figure 6 Density contours in the 3-fluid rising-bubble problem.

The Reynolds number for cases 1, 2, and 3 are 8267.43, 82.67, and 82.67, respectively. The larger the Reynolds number, the more distortion the bubble should experience. The second case employs higher dynamic viscosities than the other cases, thereby decreasing the Reynolds number. Figure 6 shows that the bubble is subject to less distortion for Case 2. A comparison between the results of Case 1 (left column) and Case 3 (right column) shows the effects of surface tension. In the results of Case 3, it can be seen that the bubble doesn't split up because of the enlarged surface tension relative to Case 1. For Case 3, Figure 6 shows that the bubble eventually becomes fully immersed in the fluid of phase 2.

Concluding remarks

The PHOENICS VOF option has been extended to simulate flows involving three different immiscible fluids. The implementation has been verified successfully for the two-phase system of a bubble rising through a column of liquid. A three-phase system was also investigated by observing the behaviour of a bubble rising in a column with two stratified liquids. The bubble motion and distortion were studied qualitatively in response to changes in the physical properties of each fluid. Future work will be aimed at quantitative verification of a three-phase system by comparison with published numerical results.

References

J.U.Brackbill, D.B.Kothe, C.Zemach,"A continuum method for modeling surface tension", J. Comp. Physics 100, 335-354 (1992).

L.Gamet, J.Roenby, M.Scala, H.Zehara, "Quantitative benchmark of a single rising bubble using VOF methods", 13th Open Foam Workshop, June 24—29, Shanghai, China, (2018).

C.Hirt, B.Nicols, "Volume of fluid (VOF) method for dynamics of free boundaries", J. Comp. Physics Vol.39, No.1, 201-225 (1981).

S.Hysing, S.Turek, D.Kuzmin, N.Parolini, E.Burman, S.Ganesan & L.Tobiska, "Quantitative benchmark computations of two-dimensional bubble dynamics. Int. J. Numer. Meth. Fluids Vol.60, No.11, 1259–1288 (2009) (see also http://www.featflow.de/en/benchmarks/cfdbenchmarking/bubble.html)

R. LeVeque and Z. Li, Immersed interface methods for stokes flow with elastic boundaries or surface tension. *SIAM J. Sci. Comp.* 18 (1997), No. 3, 709–735.

S. Osher, J. A. Sethian, "Fronts propagating with curvature-dependent speed: Algorithms based on Hamilton-Jacobi formulations," J. Comp. Phys., vol. 79, no. 1, pp. 12 – 49, (1988).

N. Tofighi, M. Yildiz, "Numerical simulation of single droplet dynamics in three-phase flows using ISPH", Computers & Mathematics with Applications 66 (2013) 525‒536, (2013).